



Influence of Zn/O ratio on structural, electrical and optical properties of ZnO thin films fabricated by plasma-assisted molecular beam epitaxy

Bingye Zhang^{a,b}, Bin Yao^{a,c,*}, Shuangpeng Wang^{a,b}, Yongfeng Li^{a,b}, Chongxin Shan^a, Jiying Zhang^a, Binghui Li^a, Zhenzhong Zhang^a, Dezhen Shen^a

^a Key Laboratory of Excited State Process, Chinese Academy of Science, Changchun Institute of Optics, Fine Mechanics and Physics, Changchun 130033, People's Republic of China

^b Graduate School of Chinese Academy of Sciences, Beijing 100039, People's Republic of China

^c Department of Physics, Jilin University, Changchun 130023, People's Republic of China

ARTICLE INFO

Article history:

Received 4 March 2010

Received in revised form 19 April 2010

Accepted 25 April 2010

Available online 6 May 2010

Keywords:

ZnO

Stoichiometric

Electrical properties

Optical properties

ABSTRACT

High quality ZnO films were grown on c-plane sapphire (c-Al₂O₃) substrates by plasma-assisted molecular beam epitaxy (P-MBE). The influence of Zn/O ratio on the epitaxial growth of ZnO is investigated. Via adjusting Zn/O ratio, structural, electrical and optical properties of the ZnO thin films are significantly improved, and the highest quality ZnO film with the full width of half maximum (FWHM) of 0.05° at the (002) peak and electron mobility of 54 cm²/V s is obtained at the Zn/O ratio of 1.03. When the Zn/O ratio is diverged from 1.03, the films exhibit rough surface with reticulated nanostructures. The formation mechanism of the ZnO nanostructure at non-stoichiometric condition is discussed. It is also found that both Zn-rich and O-rich samples show D⁰X emission peak located at 3.362 eV in the PL-spectra. By using the photon energy of the D⁰X and the Haynes' rules, the ionization energy of the donor corresponding to the D⁰X is calculated to be 36 meV, which implies that the D⁰X is related to hydrogen donor.

© 2010 Elsevier B.V. All rights reserved.

1. Introduction

As a wide gap semiconductor, ZnO comes to the forefront and becomes a new potential candidate for optoelectronic devices in the UV region in the present decade, due to its direct wide band gap of 3.37 eV and large exciton binding energy of 60 meV [1,2]. It is necessary to obtain high quality ZnO thin films with low residual carrier concentration and defects density to realize high-performance devices [3,4]. However, preparation of high quality ZnO thin films are still difficult due to the unsuitable substrates and large number of intrinsic defects, impurities and dislocations introduced during growth, such as oxygen vacancies (V_O), interstitial zinc atoms (Zn_i), and hydrogen, etc. In order to resolve these problems, various deposition techniques, such as MBE, MOCVD, Magnetron sputtering, PLD, etc., have been used to obtain high quality ZnO thin films recent decades [5–9]. Among these growth techniques, molecular beam epitaxy (MBE) is proved to be the optimal method due to its ultra-high vacuum condition and high controllability. On the other hand, great efforts have been made to improve the quality of the ZnO layers with the help of the low temperature buffer layers [10], polarity control [11], and control-

ling flux ratio of the elemental sources [12]. It is well known that the flux ratio of elemental sources plays an important role in the growth of the compound semiconductors, for example, it has been demonstrated that Ga/N ratio has a strong influence on the surface morphology and optical properties of GaN film [13]. However, only a few literatures [12,14] are reported on the influence of the stoichiometry on the surface morphology and optical properties in the recent years, the effect of the Zn/O ratio on crystal quality and physical properties of ZnO film is lack systemic investigations.

In this work, ZnO films were grown on c-Al₂O₃ substrate by P-MBE at various Zn/O ratios. The influence of Zn/O ratio on the structural, electrical and optical properties of the ZnO films was investigated.

2. Experimental details

High quality ZnO films were grown on c-Al₂O₃ substrates by P-MBE at various Zn/O ratios. For the removal of surface contamination as well as the mechanical polishing damaged surface layer, the Al₂O₃ (0001) substrates were degreased in acetone and ethanol for 10 min, respectively, and then chemically etched for 15 min in a hot solution of H₂SO₄:H₃PO₄ = 3:1 at 160 °C, followed by a rinse in deionized water. Elemental zinc with 99.9999% in purity was used as a mean of a Knudsen effusion cell. To get atomic oxygen, research grade O₂ (99.999%) was activated by an Oxford Applied Research Model HD 25 rf (13.56 MHz) plasma source operated at a power of 300 W. The growth temperature and the chamber pressure were kept at 800 °C and 1 × 10⁻⁵ mbar, respectively. The thickness of all the epitaxial films was 400 nm. All experiments were carried out in the same condition except the Zn source temperature was altered from 215 °C to 250 °C with an interval of 5 °C.

* Corresponding author at: No. 3888, Dong Nanhu Road, Changchun 130033, People's Republic of China. Tel.: +86 431 86176355; fax: +86 431 85682964.

E-mail addresses: yaobin196226@yahoo.com.cn, melody402@163.com (B. Yao).

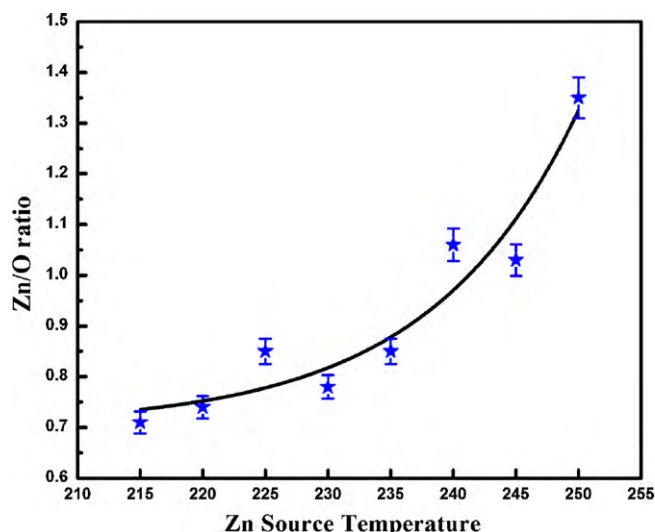


Fig. 1. Zn/O ratio of ZnO films as a function of the Zn source temperature.

Surface morphology of the ZnO films was studied by field-emission scanning electronic microscope (FESEM). Energy dispersive spectroscopy (EDS) was used to determine the content of Zn and O of the ZnO films. Rigaku O/max-RA X-ray system using $\text{CuK}\alpha$ ($\lambda = 1.5418 \text{ \AA}$) was used to investigate the orientation of the ZnO films. Hall-effect measurements were performed to analyze the electrical properties of the sample in Van de Pauw configuration by Lake Shore's 7707 Hall measurement system. The PL-spectra of the ZnO films was measured by a He–Cd laser with a wavelength of 325 nm.

3. Results and discussion

Fig. 1 shows the Zn/O ratio of the ZnO thin films as a function of Zn source temperature in the present work. As shown in Fig. 1, the Zn/O ratio increases exponentially from 0.71 to 1.35 as Zn source temperature increases from 215 °C to 250 °C, implying that the composition of the ZnO film changes as Zn source temperature is raised.

Fig. 2 shows the SEM images of the surface morphology of the ZnO films at different Zn/O ratio. It is found from the SEM images

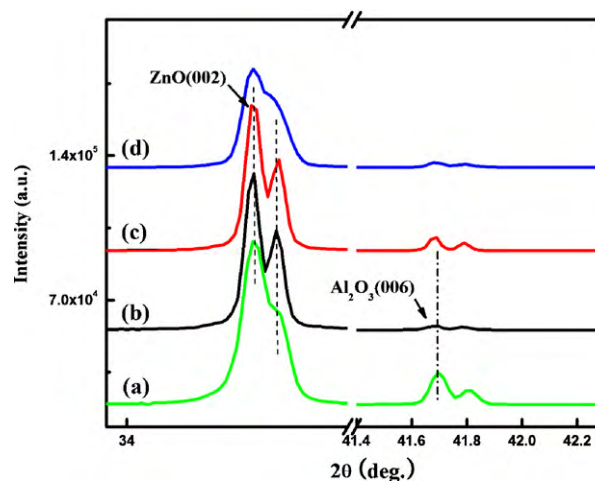


Fig. 3. The XRD patterns of ZnO films grown at Zn/O ratios of (a) 0.71, (b) 0.78, (c) 1.03 and (d) 1.35.

that reticulated structures and irregular steps are formed on ZnO layers grown under O-rich condition, as shown in Fig. 2(a) and (b). As the Zn/O ratio increases to the stoichiometric condition, reticulated structures disappear and the step edge becomes regular. When Zn/O ratio moves to Zn-rich condition, hexagonal pits can be observed on the surface, as shown in Fig. 2(d). The result implies that the surface morphology of the ZnO is related to the Zn/O ratio. When the Zn/O ratio is closed to stoichiometric ratio of 1:1, the ZnO film has a smooth and compact surface. The formation of reticulated structures and hexagonal pits can be explained by the large mismatch between ZnO and c- Al_2O_3 . It is well known that ZnO and c- Al_2O_3 have large thermal mismatch and the lattice mismatch, which makes the ZnO film grown on c- Al_2O_3 substrate subject to large biaxial stress. When the ZnO film is fabricated at non-stoichiometric ratio, there exist excessive zinc or oxygen atoms in the ZnO film. A previous literature [15] indicates that the excessive Zn or O driven by the biaxial stress can move to the surface and produce a lot of defects at the surface, leading to the formation of rough surface with reticulated structures. However, when the ZnO

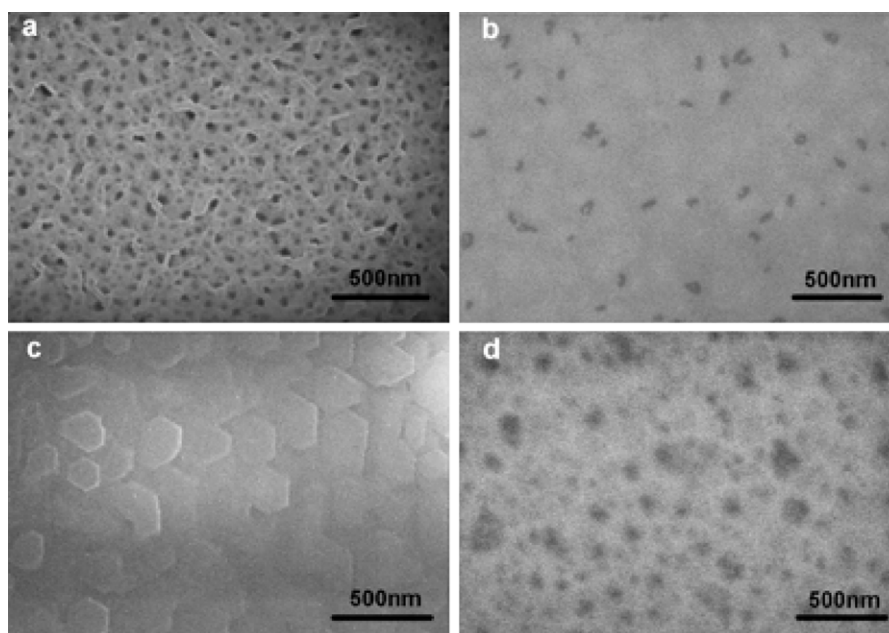


Fig. 2. The SEM images of ZnO films grown at Zn/O ratios of (a) 0.71, (b) 0.78, (c) 1.03 and (d) 1.35.

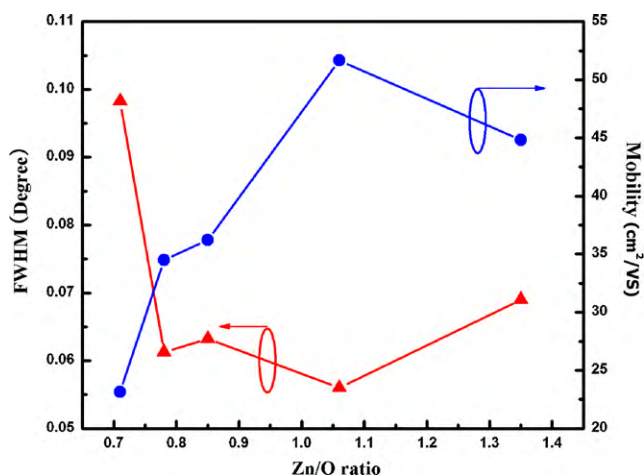


Fig. 4. The FWHM and mobility of ZnO films as function of Zn/O ratio.

film is grown near stoichiometric ratio of 1:1, Zn and O atoms are bound with each other in the ZnO film. Excessive Zn or O atoms are few in the ZnO film, which makes surface defects decrease and the surface smooth and compact.

Fig. 3 shows the XRD patterns of ZnO films with the different Zn/O ratios (a) 0.71, (b) 0.78, (c) 1.03, (d) 1.35, respectively. Besides the diffraction peak of the Al₂O₃ (006) at 41.68°, it is clearly found in Fig. 3 that only ZnO (002) diffraction peak is observed at 34.4°, indicating that all the films have a wurtzite structure with *c*-axis preferential orientation. All the (002) peaks consist of two peaks, which are assigned to the different radiation wavelength of CuKα₁ and CuKα₂, implying that the films have good crystal quality. The FWHM of the ZnO film with various Zn/O ratios are measured and plotted in Fig. 4, indicating that the FWHM changes with the Zn/O ratios. It could be also found in Fig. 3 that the intensity and FWHM of the ZnO film is stronger and narrower as the Zn/O ratio is closed to 1:1 (sample (a)–(c)), which indicates that the crystal quality of ZnO films becomes better. When the Zn/O ratio is diverged from 1:1, the intensity and FWHM become weaker and broader again (sample (d)). The strongest intensity and narrowest FWHM (0.05°) occur at the Zn/O ratio of 1.03. According to the Scherrer formula, we know that the crystalline grains in sample (c) are bigger than those in other samples, which means that the highest crystal quality ZnO films can be fabricated at stoichiometric growth condition.

The evolution of the FWHM and mobility variation of the ZnO films at different Zn/O ratios is plotted in Fig. 4. It clearly shows that the value of the FWHM goes down and then up from 0.10° to 0.07°, and reach the smallest (0.05°) at the Zn/O ratio of 1.03. The Hall-effect of the samples is also measured under various Zn/O ratios, the mobility increases significantly from 18 cm²/V s to 54 cm²/V s. It can be explained by the decrease in number of the carrier-scattering boundaries [16]. This result indicates that the grain grows larger by choosing the appropriate Zn/O ratio in the growth of ZnO thin films, which agrees with the results of SEM and XRD nicely.

Fig. 5 shows normalized low temperature (80K) photoluminescence spectra of the samples with different Zn/O ratios in a logarithmic scale. It can be seen from Fig. 5 that all the samples show strong UV emissions. The dominant peak located at 3.362 eV is assigned to the radiative recombination of excitons bound to a neutral donor (D⁰X) [17], and this dominant PL peak has a shoulder at 3.37 eV, which is assigned to the free exciton (FX_A) emission. The peaks at 3.312 eV, 3.235 eV, 3.163 eV and 3.089 eV are assigned to the first, second, third, and fourth phonon replicas of free exciton, respectively, since the energy difference between the FX_A and the FX_A LO bands is equal to the energy of the optical phonon of ZnO

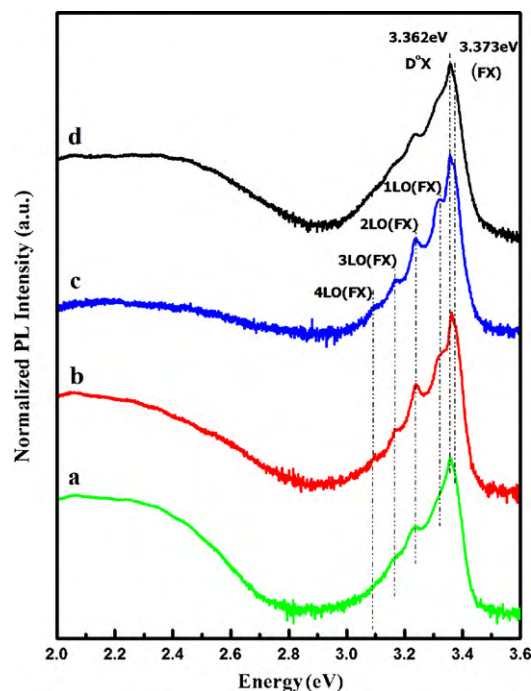


Fig. 5. Normalized PL-spectra of ZnO films grown under Zn/O ratios of (a) 0.71, (b) 0.78, (c) 1.03 and (d) 1.35 at 80K.

(72 meV) [18]. Sample (c) shows the weakest deep level emission, which proves the highest crystal quality of ZnO films. These results are consistent with the results of XRD and SEM.

It should be noted that both Zn-rich and O-rich samples show the same D⁰X emission peak position in the PL-spectra. The origin of the D⁰X emission in ZnO is not well understood yet. As can be seen in other literature, most of the ZnO films exhibit the D⁰X emission around 3.36 eV commonly. In order to clarify the origin of D⁰X emission, we correlate the binding energies ($E_{FX} - E_{D^0X}$) of the excitons bond to the neutral donors with the donor ionization energies E_D . This correlation is originally formulated by Haynes' rule [19]. According to the Haynes' rules, the donor ionization energy E_D can be expressed by

$$E_D = \frac{(E_{FX} - E_{D^0X})}{\alpha},$$

where E_{FX} is the free exciton transition energy, E_{D^0X} is the energy of excitons bound to a neutral donor, α is the Haynes' factor. Fig. 5 shows free exciton transitions at 3.373 eV and the donor bound exciton transitions (D⁰X) at 3.362 eV, the calculated Haynes' factor is 0.3 [19], which is much higher than the commonly expected value of 0.2 for similar II–VI materials. From these energies, the donor ionization energies E_D can be calculated to be 36 meV. Recent magnetic resonance experiments have shown that this donor is very likely to be hydrogen [20].

4. Conclusions

ZnO films were grown on *c*-sapphire (0001) by oxygen plasma-assisted MBE, their crystal quality and electrical, optical properties can be improved by adjusting Zn/O ratio. A high quality ZnO film with the FWHM of 0.05° and electron mobility of 54 cm²/V s is obtained at Zn/O ratio of 1.03. Diverging from this ratio, the surface of the ZnO film becomes rough, which can be attributed to the in-plane strain. D⁰X emission peaks are observed at 3.362 eV in PL-spectra of both Zn-rich and O-rich ZnO films, and the ionization energy of the donor corresponding to the D⁰X is estimated to

be 36 meV by using Haynes' rule, which implies that the donor is likely to be hydrogen.

Acknowledgements

This work is supported by the Key Project of National Natural Science Foundation of China under Grant no. 50532050, the "973" program under Grant no. 2006CB604906, the Innovation Project of Chinese Academy of Sciences, the National Natural Science Foundation of China under Grant nos. 6077601, 60506014, 10674133, 60806002 and 10874178, Swedish Research Links via VR.

References

- [1] D.C. Look, *Mater. Sci. Eng. B* 80 (2001) 383–387.
- [2] D.M. Bagnall, Y.F. Chen, Z. Zhu, T. Yao, S. Koyama, M.Y. Shen, T. Goto, *Appl. Phys. Lett.* 70 (1997) 2230–2232.
- [3] S.J. Jiao, Z.Z. Zhang, Y.M. Lu, D.Z. Shen, B. Yao, J.Y. Zhang, B.H. Li, D.X. Zhao, X.W. Fan, Z.K. Tang, *Appl. Phys. Lett.* 88 (2006) 031911.
- [4] A. Tsukazaki, T. Onuma, M. Ohtani, T. Makino, M. Sumiya, K. Ohtani, S.F. Chichibu, S. Fuke, Y. Segawa, H. Ohno, H. Koinuma, M. Kawasaki, *Nat. Mater.* 4 (2005) 42–46.
- [5] H. Lin, S. Zhou, H. Teng, T. Jia, X. Hou, S. Gu, S. Zhu, Z. Xie, P. Han, R. Zhang, *J. Alloys Compd.* 479 (2009) L8–L10.
- [6] G.Z. Xing, B. Yao, C.X. Cong, T. Yang, Y.P. Xie, B.H. Li, D.Z. Shen, *J. Alloys Compd.* 457 (2008) 36–41.
- [7] Sang Mo Yang, Seok Kyu Han, Jae Wook Lee, Jung-Hyun Kim, Jae Goo Kim, Soon-Ku Hong, Jeong Yong Lee, Jung-Hoon Song, Sun Ig Hong, Jin Sub Park, Takafumi Yao, *J. Cryst. Growth* 312 (2010) 1557–1562.
- [8] T. Prasada Rao, M.C. Santhosh Kumar, S. Anbumozhi Angayarkanni, M. Ashok, *J. Alloys Compd.* 485 (2009) 413–417.
- [9] J.-H. Kim, D.-H. Cho, W. Lee, B.-M. Moon, W. Bahng, S.-C. Kim, N.-K. Kim, S.-M. Koo, *J. Alloys Compd.* 489 (2010) 179–182.
- [10] M.S. Kim, T.H. Kim, D.Y. Kim, et al., *J. Cryst. Growth* 311 (2009) 3568–3572.
- [11] Z.-Q. Yufeng Dong, D.C. Fang, G. Look, J. Cantwell, J.J. Zhang, L.J. Song, Brillson, *Appl. Phys. Lett.* 93 (2008) 072111.
- [12] A. Setiawan, Z. Vashaei, M. Whan Cho, T. Yao, *J. Appl. Phys.* 96 (2004) 3763–3768.
- [13] E.J. Tarsa, B. Heying, X.H. Wu, P. Fini, S.P. Den Baars, J.S. Speck, *J. Appl. Phys.* 82 (1997) 5472–5479.
- [14] H.-J. Ko, T. Yao, Y. Chen, S.-K. Hong, *J. Appl. Phys.* 92 (2002) 4354–4360.
- [15] Y.F. Li, B. Yao, Y.M. Lu, C.X. Cong, Z.Z. Zhang, Y.Q. Gai, C.J. Zheng, B.H. Li, Z.P. Wei, D.Z. Shen, X.W. Fan, *Appl. Phys. Lett.* 91 (2007) 021915.
- [16] T. Ohgaki, N. Ohashi, H. Kakemoto, S. Wada, Y. Adachi, H. Haneda, T. Tsurumi, *J. Appl. Phys.* 93 (2003) 1961–1965.
- [17] B.K. Meyer, H. Alves, D.M. Hofmann, W. Kriegseis, D. Forster, F. Bertram, J. Christen, A. Hoffmann, M. Straßburg, M. Dworzak, U. Haboeck, A.V. Rodina, *Phys. Status Solidi (b)* 241 (2004) 231–260.
- [18] D.C. Reynolds, D.C. Look, B. Jogai, R.L. Jones, C.W. Litton, W. Harsch, G. Cantwell, *J. Lumin.* 82 (1999) 173–176.
- [19] H. Alves, D. Pfisterer, A. Zeuner, T. Riemann, J. Christen, D.M. Hofmann, B.K. Meyer, *Opt. Mater.* 23 (2003) 33–37.
- [20] D.M. Hofmann, A. Hofstaetter, F. Leiter, H. Zhou, F. Henecker, B.K. Meyer, *Phys. Rev. Lett.* 88 (2002) 045504.